

# 集中横荷重を受ける中空鋼管部材の全体たわみ挙動に及ぼす加力点の局部変形の影響に関する解析的研究

エフェンディ, マハムド コリ  
九州大学大学院人間環境学府空間システム専攻 : 博士後期課程

河口, 弘光  
九州大学大学院人間環境学府空間システム専攻 : 博士後期課程

河野, 昭彦  
九州大学人間環境学研究院都市・建築学部門

蜷川, 利彦  
九州大学人間環境学研究院都市・建築学部門

他

<https://doi.org/10.15017/1515828>

---

出版情報 : 都市・建築学研究. 26, pp.79-90, 2014-07-15. Faculty of Human-Environment Studies, Kyushu University

バージョン :

権利関係 :

# 集中横荷重を受ける中空鋼管部材の全体たわみ挙動に及ぼす加力点の 局部変形の影響に関する解析的研究

An Analytical Study on the Effect of Local Deformation at Loading Point on Overall Flexural Deformation Behavior in Steel Tubular Member Subjected to Concentrated Lateral Load

マハムド コリ エフエンディ\*, 河口弘光\*, 河野昭彦\*\*

蜷川利彦\*\*, 松尾真太郎\*\*, 津田恵吾\*\*\*, 城戸將江\*\*\*

Mahmud Kori EFFENDI\*, Hiromitsu KAWAGUCHI\*, Akihiko KAWANO\*\*,  
Toshihiko NINAKAWA\*\*, Shintaro MATSUO\*\*, Keigo TSUDA\*\*\* and Masae KIDO\*\*\*

Tsunami debris attacked and destroyed many buildings in the 2011 off the Pacific coast of Tohoku Earthquake. Steel tubular members are popularly used for the beam-columns of buildings in Japan, so that an evaluation method of the resistant capacity of the member against Tsunami debris becomes the urgent problem. One of the difficulties to develop the evaluation method is that the local deformation caused by the collision object degrades the overall strength of a steel tubular member which degrading rate may be changed by the contact tip shape of the object. In order to investigate the effects, we conducted a static nonlinear analysis of steel tubular members subjected to concentrated lateral loads by using the finite element analysis (FEM) program MSC Marc. The accuracy of the FEM analysis model is verified by the experiment. Being based on the parametric numerical study, it is discussed the degrading effect of loading tip shapes on the lateral load-deflection relations and the collapse modes of steel tubular members.

*Keywords: Steel Tubular Members, Static Loading, FEM Analysis, Tip Shapes of Loading*  
鋼管部材、静的載荷、有限要素法、加力部先端形状

## 1. Introduction

Aftermath of the 2011 off the Pacific coast of Tohoku Earthquake let us reconfirm the importance of the vertical evacuation buildings or facilities in the low ground areas near offshore. The steel tubular members have gained in popularity in building beam-columns in Japan, so that it should be considered that the many vertical evacuation buildings and facilities are made of steel tubular beam-columns. The structures are not enough for resisting the Tsunami wave pressure but for resisting drifting articles by Tsunami (Tsunami debris). With respect to the wave pressure, the structural design method has been already proposed by the Ministry of Land, Infrastructure and Transport in Japan. However, the rational design method has not been proposed for Tsunami debris so far. Therefore the evaluation method of the resistant capacity of the steel tubular members against Tsunami debris becomes the urgent problem. One of the difficulties to derive the evaluation method is that the flexural behavior of a steel tubular member is degraded by the local deformation in tubular wall by the collision of Tsunami debris, where the degrading rate depends on the contact tip shape of the article.

There is not the systematic study of this field as far as we know it. Therefore, we conducted a static nonlinear analysis of steel tubular members subjected to concentrated lateral loads by using the finite element method (FEM) program MSC Marc. Analytical models are three dimensional FEM models taking the account of the material and the geometrical nonlinearity in order to predict the flexural behaviors with local deformations of steel tubular members. Exactly speaking, the impact problem should be treated by a dynamic analysis. However, the expectable velocity of Tsunami debris may 7 m/second at the most. In such a low speed collision, the static analysis can express the fundamental deformation behaviors of the steel tubes except for the increases of material yield stresses by the strain rate.

The shapes of loading tips and the shapes of tubular cross sections are the analytical parameters in this parametric numerical study.

## 2. Analysis by Finite Element Method

### 2.1 Outline of Analysis Method

The MSC Marc<sup>1)</sup>, a general purpose finite element

\* 空間システム専攻博士後期課程

\*\* 都市・建築学部門, 九州大学

\*\*\* 国際環境工学部, 北九州市立大学

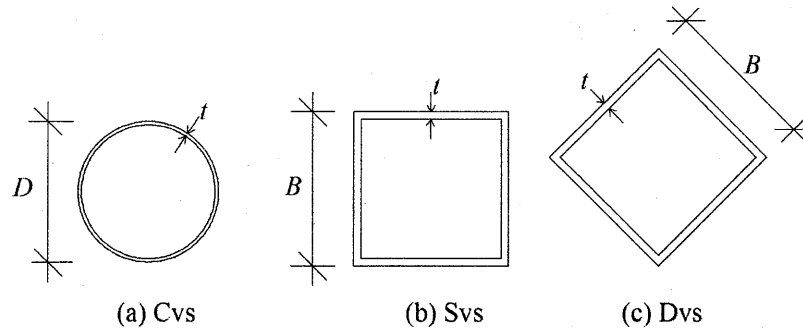


Fig. 1 Cross Sections of Tubular Members

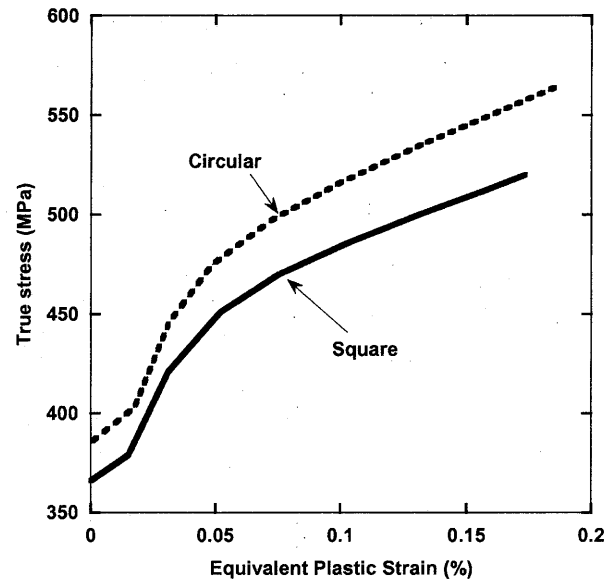


Fig. 2 Equivalent Plastic Strain and True Stress Relationships

Table 1 Dimensions and material properties of Steel Tubes

Cross-section	Steel Tube	$D$ or $B$ (mm)	$t$ (mm)	$f_y$ (N/mm <sup>2</sup> )	$f_u$ (N/mm <sup>2</sup> )	$E_s$ (N/mm <sup>2</sup> )	$Z_p$ (cm <sup>3</sup> )	$\epsilon_y$ (%)
Circular	STK400	114.3	3.2	386	564	211000	39.5	0.194
Square	STKR400	100.0	3.0	366	520	189000	43.7	0.193
Diamond							40	

Table 2 Specimens and experimental parameter

Specimen	Cross-section	$D$ or $B$ (mm)	$t$ (mm)	$D/t$ or $B/t$	Span ( $L$ ) (mm)
Cvs	Circular	114.3	3.2	35.7	996
Svs	Square	100.0	3.0	33.2	996
Dvs	Diamond				

software, is used to simulate the steel tube behaviors. A pre- and post-processes are handled by the Mentat software which generates the mesh segmentations, and specifies the material and geometry assignment, loading conditions and boundary conditions. The contact option is taken into account between deformable bodies of steel tubes and rigid bodies of the loading tip. In MSC Marc, the contact option is imposed by means of the solver constraints<sup>2)</sup>. The full Newton-Raphson iterative procedure is performed to minimize the unbalance forces in each loading step.

## 2.2 Material Parameters

Circular, square and diamond shapes of cross sections

of steel tubular members are analyzed in this study as shown in Fig. 1. The diamond shape means the cross section which is turned square tube 45 degrees. The material properties of steel tubular models are specified to be same as the test specimens those had been performed in the past<sup>3)</sup>.

MSC Marc<sup>1)</sup> requires the stress and strain characteristics to be entered as the true stress and the equivalent plastic strain, respectively, as shown in Fig. 2. The von Mises yield criterion and the kinematic hardening rule are used as the plastic flow conditions.

The yield stress of square tubular members and circular tubular members of the past test specimens were

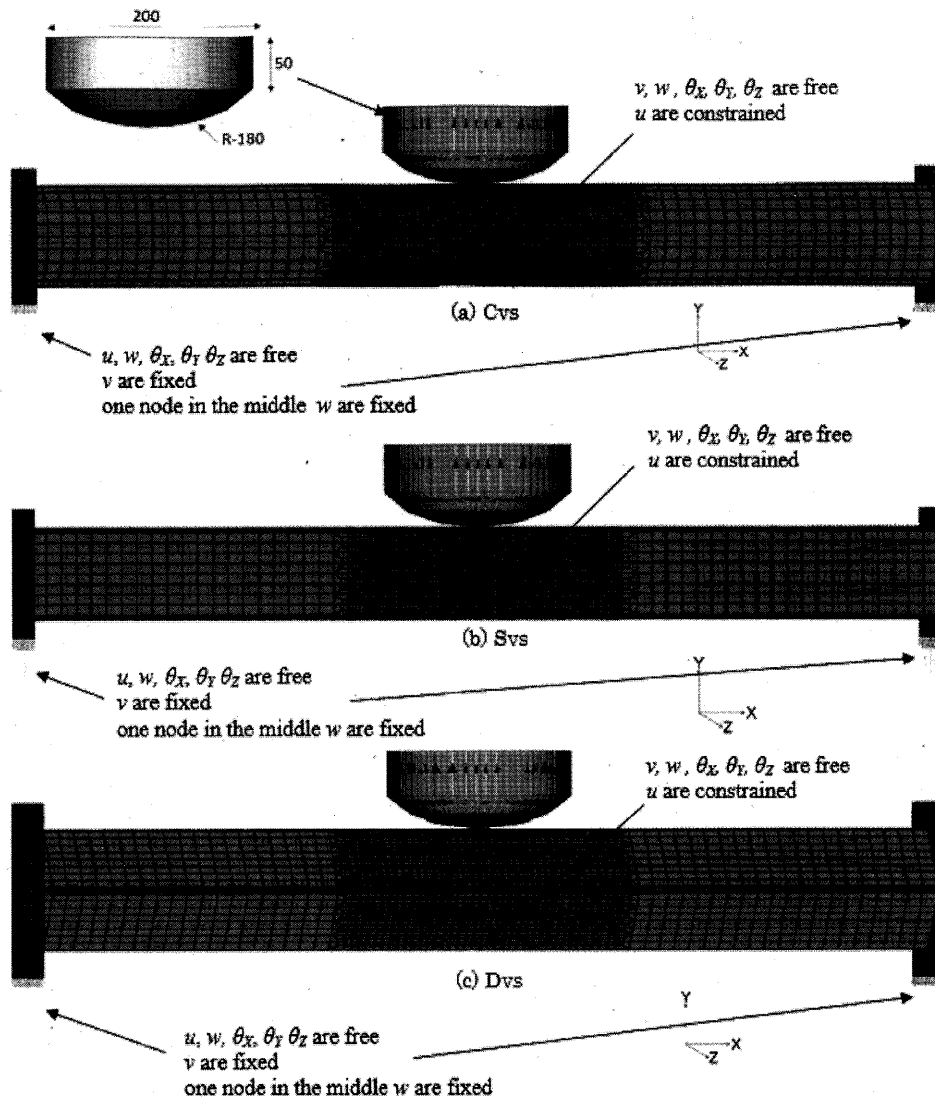


Fig. 3 Mesh Grid of Topographic Model

366 N/mm<sup>2</sup> and 386 N/mm<sup>2</sup>, respectively. The Poisson's ratio,  $\nu$  for all members is 0.3. Table 1 summarizes the dimensions and material properties of each specimen, where Cvs, Svs and Dvs is the names of specimens with circular, square and diamond steel tubular sections, respectively.  $D$  is the outside diameter of a circular steel tube,  $B$  is the one side length of square steel tube,  $t$  is thickness of a tube,  $f_y$  is the yield stress,  $f_u$  is the tensile stress,  $E_s$  is Young's modulus and  $L$  is the span length of a simple beam specimen.

### 2.3 Element Type, Boundary Conditions and Mesh Segmentation

The four-node thick shell element with six degrees of freedom per a node ( $u$ ,  $v$ ,  $w$ ,  $\theta_x$ ,  $\theta_y$  and  $\theta_z$ ) is used for the analytical model of a steel tubular member (the element type 75 of MSC Marc<sup>4</sup>).

Briefly, the supporting conditions of an analytical model are the simple beam to which the concentrated lateral load applied at the mid-span. In three dimensional spaces, where the orthogonal coordinate system  $O-X, Y, Z$  is defined

as shown in Fig. 3, the all nodes on both supports are constrained in the direction of  $Y$  axis and an additional one node in the mid of the nodes are constrained in the direction of  $Z$  axis to stabilize the analysis. The remaining degrees of freedom are set to be free.

The displacements of one node at the bottom of cross section at mid span are constrained in the direction of  $X$  axis. The loading tip, which is a rigid body composed of rigid surface elements, applies lateral loads to a steel tube which is composed of deformable shell elements. The vertical displacement of the loading tip is increased by the displacement control method. The number of rigid surface elements for the loading tip is 1080 surfaces. With respect to steel tubular members, the number of shell elements is 8480 for each of a diamond tube and a square tube, and 4896 for a circular tube. With respect to end plate, the shell elements are used with the stiff material properties of high Young's Modulus.

### 2.4 Contact Analysis

The contact interactions are considered between a rigid

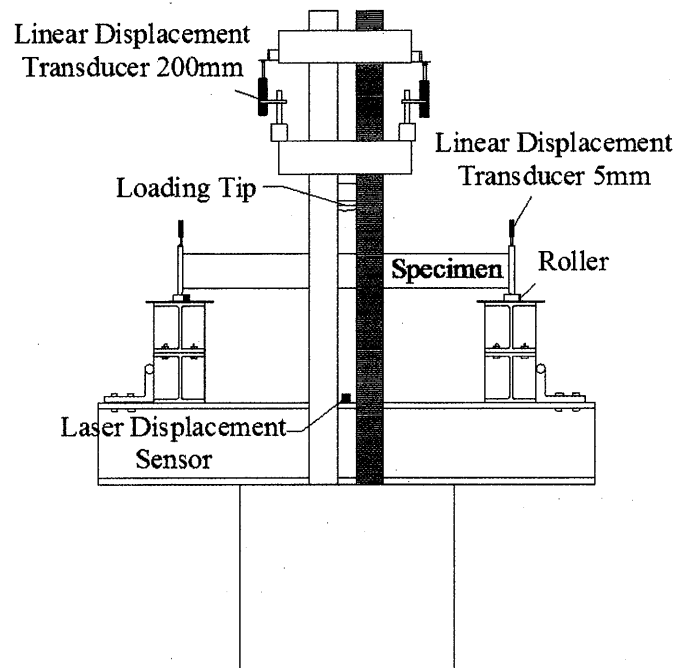


Fig. 4 Test Setup of Static Loading on Steel Tubular Member

body of the loading tip and a deformable body of steel tubular member. The contact tolerance of the deformable body is defined to be between plus and minus of 0.1 mm. The contact happens between a rigid body and a deformable body, overlapping relative displacement in the normal direction of the surface comes over the tolerance. The MSC Marc deals with the contact analysis by the direct constraint procedure.

### 3. Experimental Work

Specimens of circular tube,  $Cvs$  ( $D/t = 35.7$ ), square tube,  $Svs$  ( $B/t = 33.2$ ), and diamond tube,  $Dvs$  ( $B/t = 33.2$ ) have been tested at Kyushu University<sup>3)</sup>. The dimensions and material properties of steel tubes for test specimens can be seen in Table.1. The specimens and the experimental parameters are listed in Table 2.

The test setup for static loading is illustrated in Fig. 4. The supports are pin and roller supports at both ends. Roller support is a simple one which is just greased between the bottom end plate of a specimen and testing bed which is made by H-shaped steel, so that specimen ends can freely slide in the member axis direction.

Two displacement transducers are installed to measure the displacement of a loading head, and a laser displacement sensor is placed at bottom of mid-span of a tubular member to measure the overall displacement. The difference between the displacements of the loading head and the overall deflection indicates the local deformation,  $\delta_{LD}$  of tubular wall.

Strain gauges are installed at bottom of mid and quarter span for a square tube and a circular tube. With respect to diamond tube, strain gauges are installed at center of plate elements at lower sides at mid and quarter span.

## 4. Results and Discussions

### 4.1 Comparison of Load-Displacement Relationships between by FEM analysis and by Experiment

The load-displacement relationships of circular, square and diamond tubular members ( $Cvs$ ,  $Svs$  and  $Dvs$ , respectively) are plotted in Figs. 5, 6 and 7, respectively. The displacement is the flexural deflection measured at the bottom side of mid-span of the steel tubular member, which does not include the local deformation of steel tubular wall by the loading tip.

The initial stiffnesses and strength deterioration rates, which is the negative slope angle, by FEM analysis and by experiment are almost same. The peak load of circular tubular members by FEM analysis showed somewhat higher than that of the experiment. With respect to square and diamond tubular members, the peak load by FEM analysis underestimates that by experiment.

Although the strength deteriorates after the peak in all tubes, the deterioration rates of the square and diamond tubes are quicker and harder than that of the circular tube.

Generally speaking, the load-displacement relationships obtained by FEM analysis may be said to predict the peak loads and the deterioration rates of experimental specimens successfully.

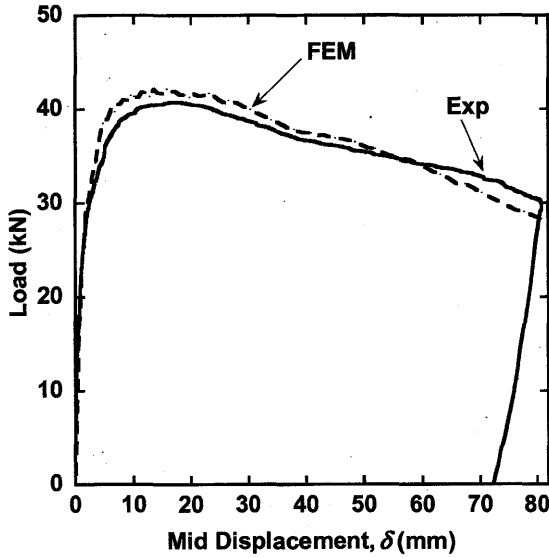


Fig. 5 Load-Displacement Relationships Between Experimental and FEM Analysis of Cvs

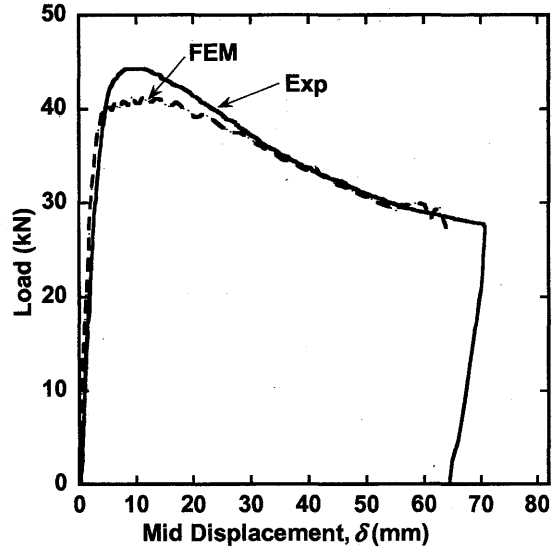


Fig. 6 Load-Displacement Relationships Between Experimental and FEM Analysis of Svs

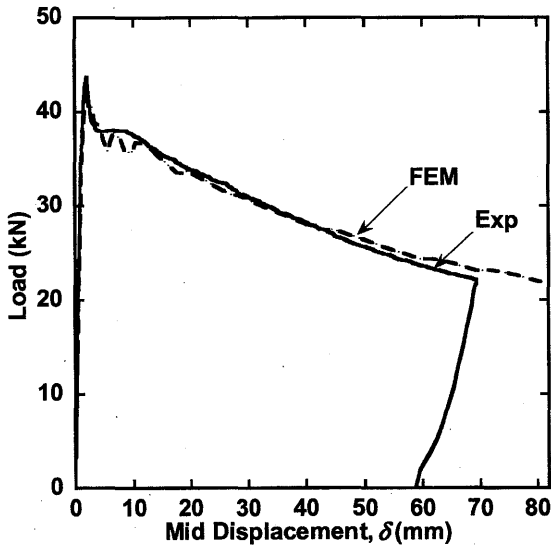


Fig. 7 Load-Displacement Relationships Between Experimental and FEM Analysis of Dvs

#### 4.2 Local Deformation of Tubes

The local deformation of a tubular wall is caused by the loading tip. Furthermore, the local buckling possibly happens in the tubular wall of members. The local buckling has not been measured in the experiment. Only the local deformation with respect to difference between the displacements of loading head and the overall displacement is obtained from the experiment. The FEM Analysis calculation of the local deformation with local buckling,  $\delta_{LB}$  (Eq. 1) and the local deformation without local buckling,  $\delta_{LD}$  (Eq. 2) can be seen in Fig. 8.

$$\text{Local deformation with local buckling, } \delta_{LB}: \\ \delta_{LB} = \delta_{ts} - \delta \quad (1)$$

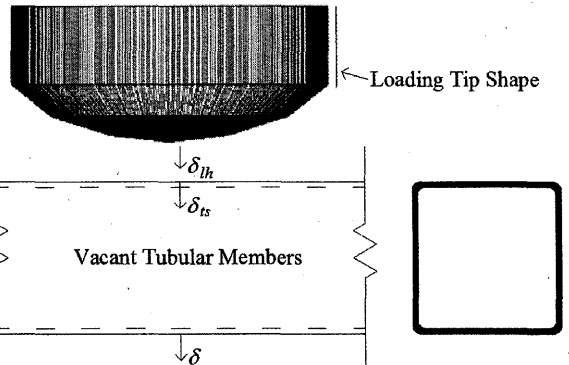


Fig. 8 Displacements at Mid-Span of FEM Analysis Model

$$\text{Local deformation without local buckling, } \delta_{LD}: \\ \delta_{LD} = \delta_{th} - \delta \quad (2)$$

where,

$\delta_{ts}$ : displacement of the top node at mid-span of a member

$\delta$ : displacement of bottom mid-span of a member

$\delta_{th}$ : displacement of head of loading tip

Generally speaking, the FEM prediction of local deformation without local buckling,  $\delta_{LD}$  of Cvs, Svs and Dvs tubular members show in good agreement with those of experiment as shown in Figs, 9, 10 and 11, respectively.

The prediction of the local buckling is obtained by the difference between  $\delta_{LB}$  and  $\delta_{LD}$ . In Svs and Dvs have the larger magnitudes of local buckling modes than that of Cvs, because the differences between  $\delta_{LB}$  and  $\delta_{LD}$  of Svs dan Dvs are found larger than that of Cvs.

#### 4.3 Comparison of Collapse Modes by FEM analysis and those by Experiment

The collapse modes by FEM analysis for Cvs (circular

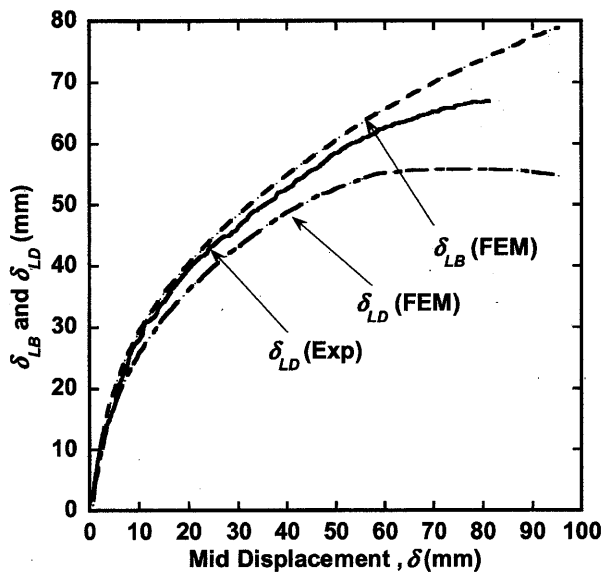


Fig. 9 Local Deformations of Cvs

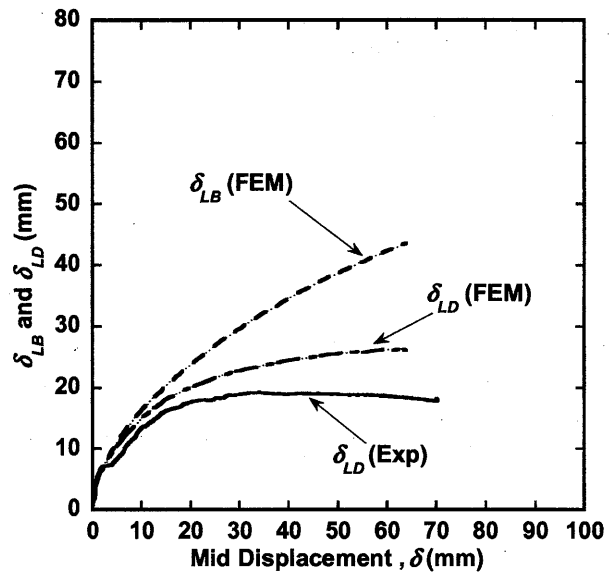


Fig. 10 Local Deformations of Svs

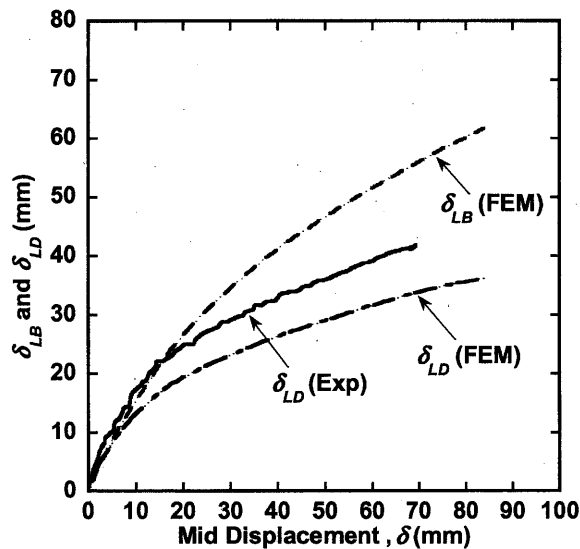


Fig. 11 Local Deformations of Dvs

tubes), Svs (square tubes) and Dvs (diamond tubes) are compared with those of experimental results are shown in Figs. 12, 13 and 14, respectively. At first loading stage, the shape of local deformation of the circular tubular member, Cvs, is almost similar as that of the loading tip. However, as the loading stage proceeds to the large deformation range, the local buckling of tubular wall appears. Because the curvature is shorter than that of the loading tip, the local buckling can be distinguished from the initial local deformation depending on loading tip shape. With respect to a square tube, Svs, and a diamond tube, Dvs, the local buckling modes are largely bent than that of the circular tube. This is the reason why the load-deflection relationships of the square and diamond tubes deteriorate earlier than that of the circular tube as mentioned in the section 4.1.

#### 4.4 Effect of Loading Tip Shapes on Load-Displacement Relationships

A parametric numerical study is performed for various shapes of loading tips, which are intended to tsunami debris tips as shown in Fig. 15. The loading tip of type 1 is small curvature with cylindrical shape in the contact surface. The tip types 2, 3 and 4 have spherical shapes and the curvatures of the contacting surfaces increase with the turn. The tip type 3 has been used for the experiment. The steel tubes of analytical models are Cvs, Svs, and Dvs, which are the same as those in the sections 4.1, 4.2 and 4.3.

Figure 16 indicates the load-displacement relationships of circular tubes, Cvs, subjected to lateral loads through loading tips from types 1 to 4. It is observed that the initial stiffness of each load-displacement relationship is almost

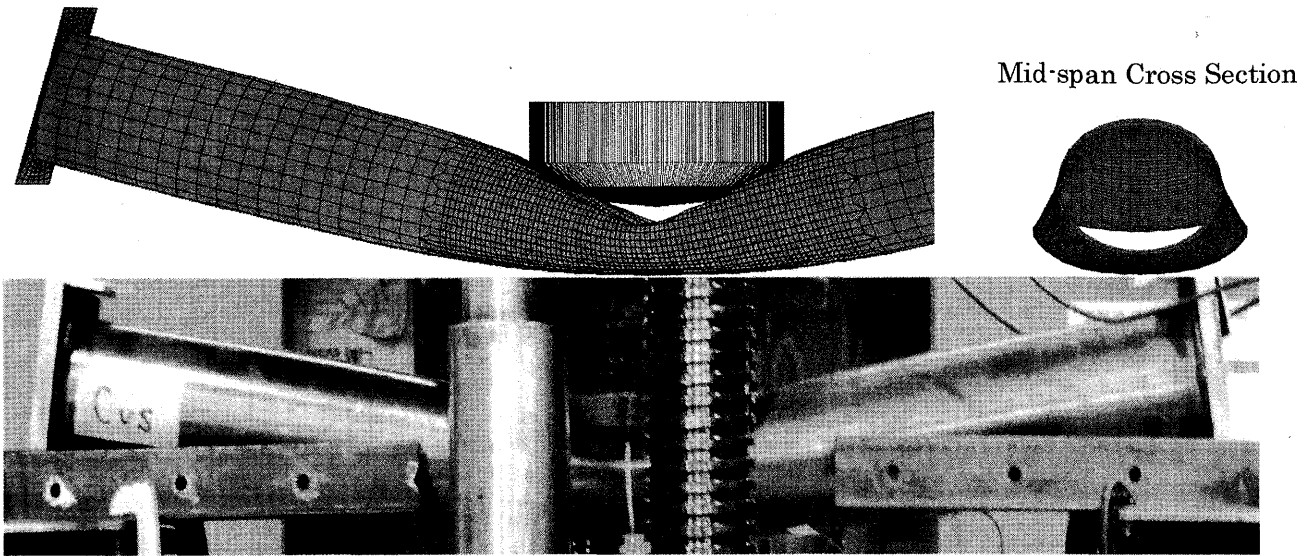


Fig. 12 Final Loading Steps: Experimental and FEM Analysis of Cvs

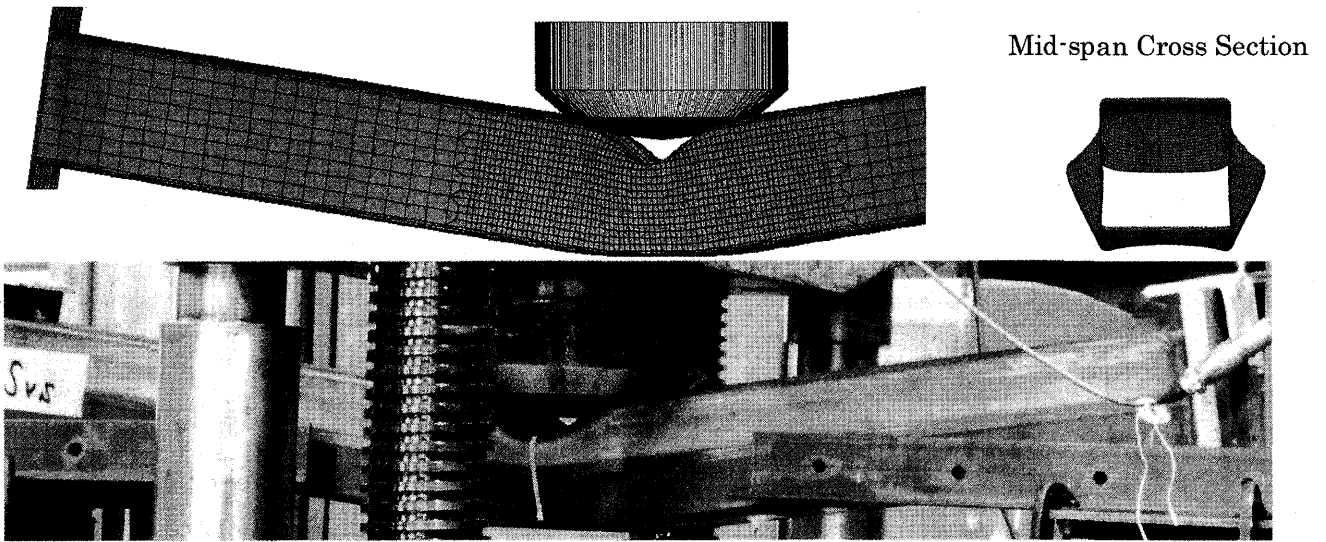


Fig. 13 Final Loading Steps: Experimental and FEM Analysis of Svs

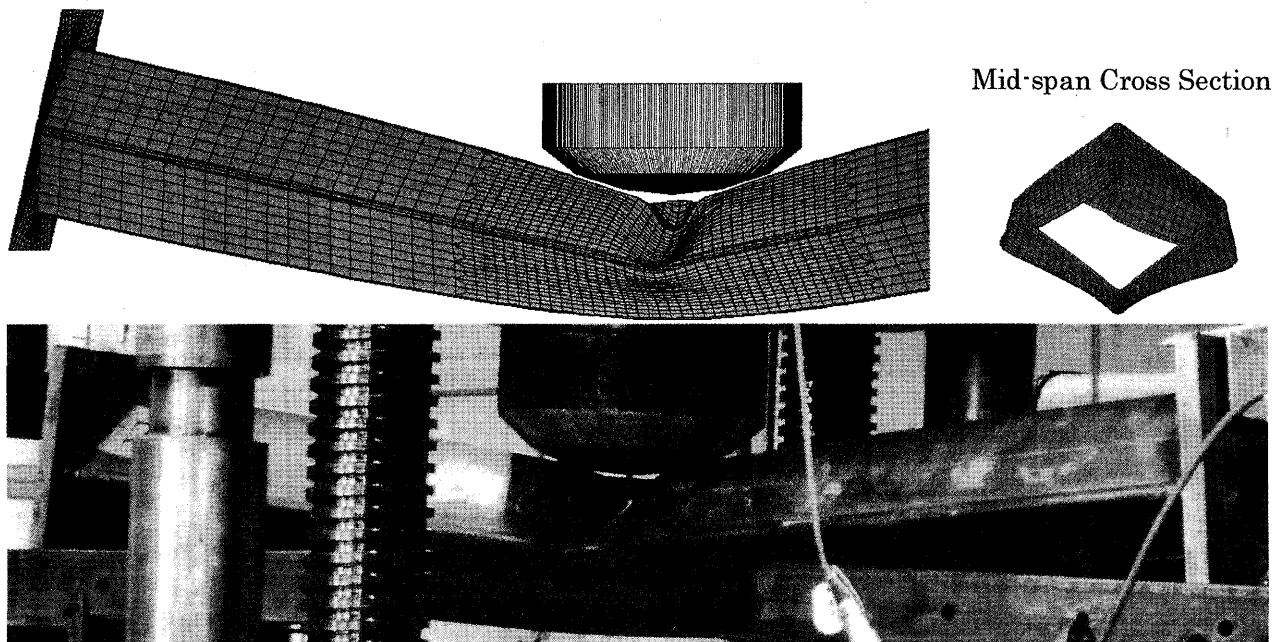


Fig. 14 Final Loading Steps: Experimental and FEM Analysis of Dvs



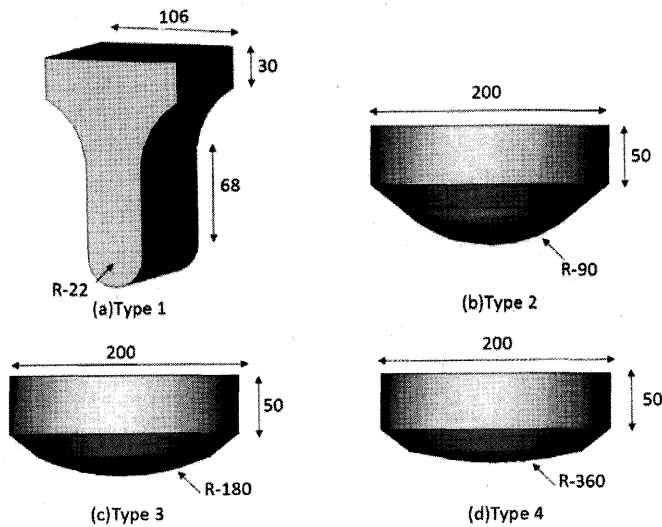


Fig. 15 Loading Tip Shapes

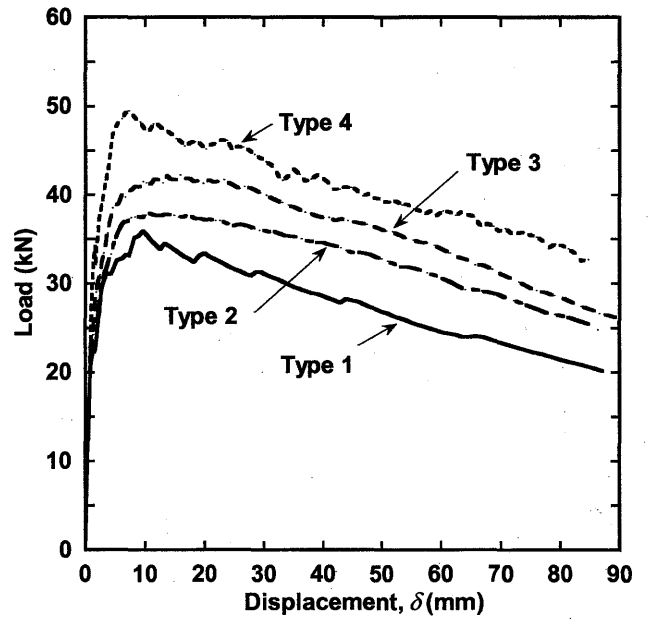


Fig. 16 Load-Displacement  $\delta$  Relationships of Cvs Under Various Loading Tip Shapes

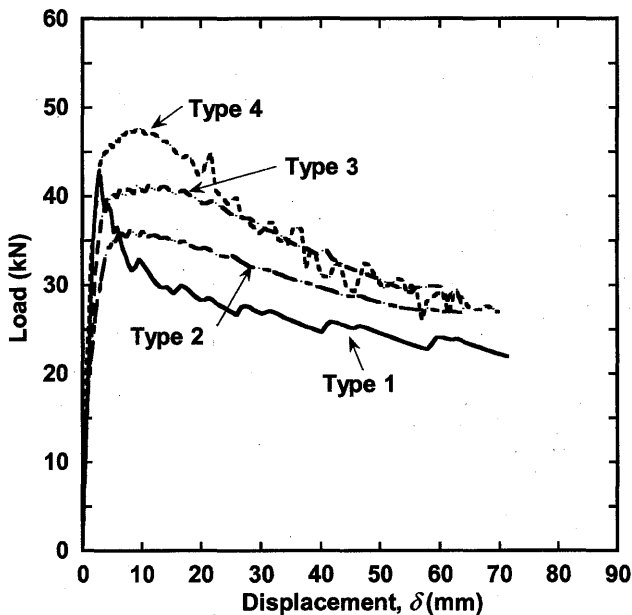


Fig. 17 Load-Displacement  $\delta$  Relationships Of Svs Under Various Loading Tip Shapes

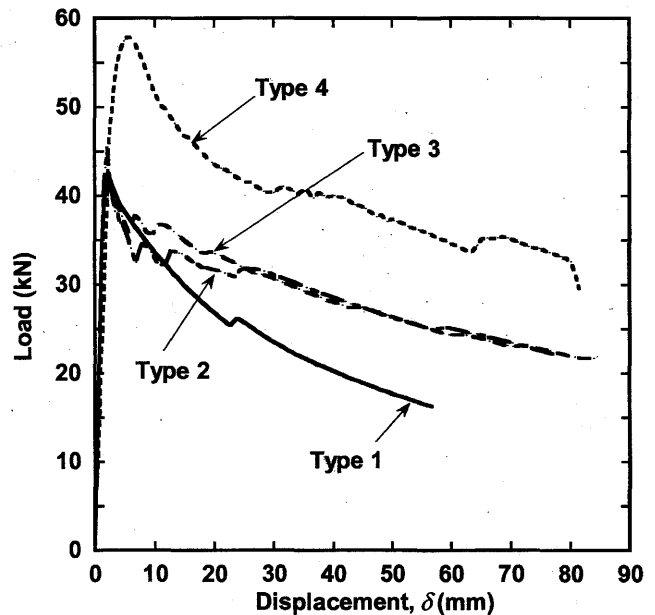


Fig. 18 Load-Displacement  $\delta$  Relationships Of Dvs Under Various Loading Tip Shapes

same, so that the loading tip shape may not affect the initial stiffness of overall flexures. The peak load increases as the curvature of loading tip increases. The negative slopes after the peaks by the tip of types 1 and 4 are somewhat steeper than those in the tip types 2 and 3.

There is somewhat fluctuation in the load-deflection relationship curve in certain parts. These fluctuations may be introduced by the determination of convergence control parameter value which must be specified to be very small value and by the complicated contact and separation processes between the rigid body and the deformable body,

which is highly influenced by the mesh size of the deformable body, so that further fine mesh size probably make the relationship curves smooth.

With respect to the square tube, Svs, in Fig. 17, the load-displacement relationship by the tip type 1 shows the quick strength deterioration after the peak load, which is quite different from those by the tip types 2 and 3. This may be explained as the curvature of cylindrical shape of the tip type 1 is smaller than the local buckling mode of the square steel tube, so that sharp tubular wall deformation happens which reduces the strength quickly. In the case of tip types 2

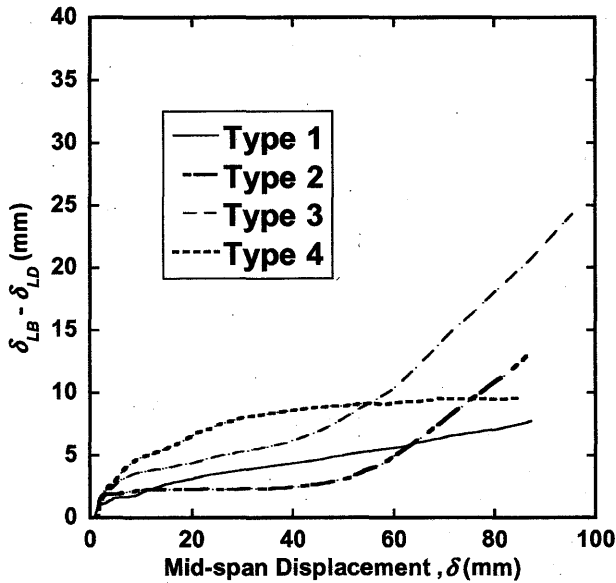


Fig. 19 Effect of Tip Shapes of Loading Toward Local Buckling of Cvs

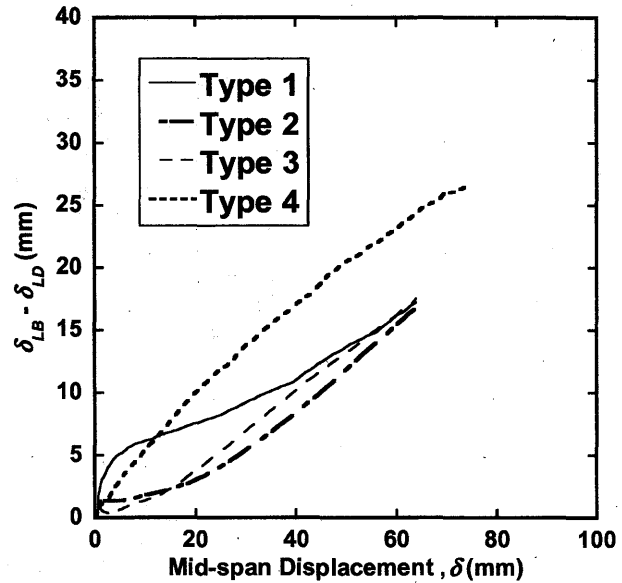


Fig. 20 Effect of Tip Shapes of Loading Toward Local Buckling of Svs

**Table 3 The comparison of plastic load of experimental and those of calculation**

Specimen	<i>D/t</i> or <i>B/t</i>	Plastic Load		<i>fP<sub>u</sub></i> / <i>cP<sub>u</sub></i>
		Theoretical	FEM analysis	
		<i>cP<sub>p</sub></i>	<i>fP<sub>p</sub></i>	
Cvs	35.7	61.2	35.6	0.6
Svs	33.2	64.2	34.3	0.5
Dvs	33.2	58.8	42.2	0.7

and 3, the load-displacement behaviors are relatively stable and the loads gradually deteriorate as the loading stages proceed. In the case of tip type 4, the peak load appears around 10 mm of  $\delta$ , which is relatively large displacement, but the strength deterioration rate is the smallest.

Quick strength deteriorations can be observed in diamond tubes for all tip types of 1 to 4 as shown in Fig. 18. This may be explained that the local buckling happens in plate elements which are not contacted with the loading tips, so that the local buckling suddenly happens when the stress exceeds the buckling stress.

The theoretical full plastic moment,  $M_p$  and plastic load,  $cP_p$  without considering local deformation for vacant steel tubular members are calculated by Eq. (3) and Eq. (4).

$$M_p = f_y Z_p \quad (3)$$

$$cP_p = \frac{4M_p}{L} \quad (4)$$

Where  $Z_p$  is the plastic modulus of a cross section

The fully plastic load, ( $fP_p$ ) of FEM analysis are determined from the horizontal projection of point of contact between load-deflection relationship curve and

one-sixth of initial stiffness of the specimens. Table 3 shows comparisons between the plastic load of the FEM analyses,  $fP_p$  and those of the calculation,  $cP_p$ .

From Figs. 16-18 shows that the tip type 1 results quick strength deterioration caused by local buckling. The strength reduction factor considering local deformation is based on tip type 2 which results the least strength in the load-displacement relationships. The reduction factor is proposed to be 50-70 % of Eq. (4).

#### 4.5 Effect of Loading Tip Shapes on Local Buckling Modes

The  $(\delta_{LB} - \delta_{LD})$  indicates the difference of the local deformation with local buckling to the one without local buckling, so that it is the magnitude of local buckling mode. The loading tip shape changes the local buckling mode and the magnitude, which affects the peak load, the deflection at the peak and the strength deterioration rate after the peak. The local buckling modes,  $(\delta_{LB} - \delta_{LD})$ , of circular tubes, Cvs, are shown in Fig. 19 for the various shapes of loading tips. The local buckling modes reach 2 - 4 mm from the initial loading stages in all cases of tip types. Therefore, the tubular wall sinks at the top of the cross section at the mid-span of a tubular member in the very early loading stage. In the cases of tip types 2 and 3, the local buckling modes indicate plateaus until around 40 mm of overall deflection  $\delta$ , and then increase again over around 50 mm of  $\delta$ . On the other hand, the local buckling modes of tip types 1 and 4 continue to increase from the initial loading stage  $\delta$ . These may be the reason that the load-displacement relationships of Cvs in the case of tip types of 1 and 4 indicate relatively quick strength

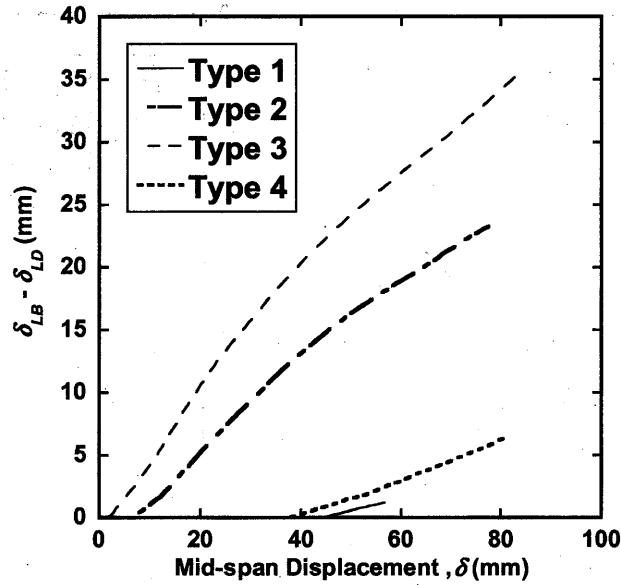


Fig. 21 Effect of Tip Shapes of Loading Toward Local Buckling of Dvs

Loading Tip Shapes	Cvs	Svs	Dvs
Type 1			
Type 2			
Type 3			
Type 4			

Fig. 22 Collapse Modes by Various Loading Tip Shapes

deteriorations as shown in Fig. 16.

Fig. 20 shows the effect of loading tip shapes on local buckling modes of square tubes, Svs. In the cases of tip types 2, 3 and 4, the local buckling modes do not appear at the initial loading stages. It may be said that the local buckling modes are harder to happen in square tubes than in circular tubes in the early loading stages except for the case of tip type 1. With respect to the case of tip types 1 and 4, the local buckling mode increases from the initial loading stage, which is quite different from those of tip types 2 and 3. This is the reason why the load-displacement relationships of the cases of tip types 1 and 4 have the sharp peak and the quick strength deterioration after the peak.

Fig. 21 shows the local buckling modes of diamond tubes, Dvs. In all cases, the  $(\delta_{LB} - \delta_{LD})$  are kept to be zero in the early loading stages, so that the top node of the mid-span of a diamond tube is subjected to intensive pressure from the loading tip. As shown in Figs.14 and 22, the local buckling of Dvs may happen at the flat plate elements around the top quadrangular corner, and then the corner also buckles as the loading stage proceeds. The load-displacement relationships in Fig. 18 indicate the sharp peaks and quick strength deteriorations.

#### 4.6 Effect of Loading Tip Shapes on Collapse Modes

Fig. 22 shows the collapse modes of steel tubes by the FEM analysis. The collapse modes of circular tubes, Cvs,

strongly depend on the loading tip shape, so that the modes are from sharp to round bending deformations of steel tubular walls, as the tip types change from No. 1 to 4. In the case of tip type 1, the circular cross section deforms into an oval shaped section in a small domain at the mid-span of the tube, which causes sharp flexural deformation of the tubular member. It may be the reason for the comparatively quick strength deterioration in the load-displacement relationship as mentioned in section 4.4.

The curvatures of tubular wall deformations of square tubes,  $S_{vs}$ , in Fig 22 indicate almost similar modes regardless of the different shapes of the loading tip types 2, 3 and 4, and they are smaller than those of the tip shapes. Therefore, the collapse modes of the square tubes in the case of tip types 2, 3 and 4 are dominated by the local buckling of steel plate elements. With respect to the case of tip type 1, a sharper bending deformation of the steel tubular wall is observed. The curvature is that of the loading tip of type 1 with the smallest curvature. This is the reason for the quicker strength deterioration in load-displacement relationships in the case of tip type 1 as shown in Fig. 17.

The collapse modes of diamond tubes,  $D_{vs}$ , in Fig. 18 indicate the complicated shapes with combined of dents by loading tips and local buckling of flat plate elements. The local buckling may happen suddenly when the stress exceeds the buckling stress, which cause the quick strength deterioration as shown in Fig. 18.

## 5. Conclusive Remarks

Conclusive remarks from the nonlinear FEM analysis investigation for tubular members subjected to concentrated lateral loads are as follows:

- (1) The three dimensional FEM analytical models of tubular members with circular, square and diamond cross sections are proposed by using thick shell elements (type No. 75, MSC Marc). The loading tip is constructed by rigid surface elements. The contact option is introduced between the tubular model and the loading tip. The analysis is proceeded by the displacement control method. The accuracy of the analytical model is successfully verified by simulating the experimental result in the past.
- (2) The parametric study is performed with the analytical parameters of tubular cross section shapes and loading tip shapes. The steel tubes are the cold-formed mild steel tubes. The diameter-to-thickness ratio of circular tubes is 35 and the width-to-thickness ratios of square and diamond tubes are 33. From the relationships between

the lateral loads and overall flexural displacements, it may be said that the initial stiffness is not changed by loading tip shapes for each tubular cross sectional shape. The shape of loading tip changes the peak load of a tubular member, which tends to increase as the curvature of loading tip shape increases. However, the degree of the change in peak load is different from each shape of tubular cross section. The strength deterioration after the peak is also affected by loading tip shapes and cross section shapes. Although the degree of strength deterioration rate depends on the combination of them, the strength deterioration in diamond tubes is harder than those of circular tubes and square tubes.

- (3) In the parametric study, the local buckling of a circular tube occurs from the initial loading stage regardless of the shapes of loading tips. On the other hand, those of a square tube and a diamond tube are none or very small at the early loading stages except for the square tube applied by loading tip type 1. However, local buckling modes grow up in square tubes as the loading stages proceed. With respect to diamond tubes, local buckling happens in flat plate elements near the top of the quadrangular corners at mid-span of members and then the corner also buckles as the loading stage proceeds.
- (4) The collapse modes of circular tubes strongly depend on the loading tip shapes, so that the mode are from sharp to round bending deformations as the curvatures of tip shape increases. With respect to square tubes, almost the same collapse modes are observed except for the case of loading tip type 1, which has the less curvature than that of the local buckling mode. The complicated shapes of the collapse modes are observed in diamond tubes with combination of dents by loading tips and local buckling of flat plate elements. The collapse mode are is different from each of loading tip shape.

The strength of vacant steel tubular members is affected by loading tip shapes. The least strength reduction factor among various loading tip shapes will be introduced in the structural design as the safe-side estimation of vacant steel tubular members against Tsunami debris. However  $D/t$  or  $B/t$  ratio may reduce the strength of vacant steel tubular members and it will be studied in the next analysis.

## 6. Acknowledgement

This study was financially supported by the Scientific Research Grant (B) H25- H27 No. 25289186, Steel structure research and educational grant project H25, Ministry of Education, Culture, Sports, Science and Technology, Japan.

One of the authors thanks the Indonesian Directorate of Higher Education Program (DIKTI) for a doctoral scholarship. The authors wish to thank the Research Institute for Information Technology, Kyushu University for the privilege of using the MSC Marc finite-element program.

#### **References**

- 1) MSC Software: MSC.MARC User's Guide, 2012
- 2) Kuijpers, AHW et al.; Finite Element Contact Analysis: Marc and Dyna3d Compared. Technische Universiteit Eindhoven, 1994
- 3) Effendi, M.K et al.: An Experimental Study on the Behavior of Concrete Filled Steel Tubular Members under Tsunami Debris Impact Load, Part 3. FEM analysis Analysis- Static Loading of Vacant Tubular Members. AIJ Kyushu branch March, 2014
- 4) MSC Software: MSC.MARC volume B element library version 2012, 2012

(受理：平成26年5月29日)